

# Evaluation of Aircraft Structures Crashworthiness Behavior using Finite Element Analysis

C. Zinzuwadia, G. Olivares, L. Gomez, H. Ly, H. Miyaki

Wichita State University, National Institute for Aviation Research, Computational Mechanics Laboratory,  
Wichita, KS 67260-0093

## Abstract

*Despite ongoing worldwide research and discussion regarding broad aspects of airplane crashworthiness, no specific dynamic regulatory requirement currently exists. However, the Federal Aviation Administration (FAA) requires an assessment of each new aircraft model to ensure that the airplane crash performance will not significantly deviate or otherwise degrade from typical dynamic characteristics found in previous designs [8]. The increased use of composite airframe structural components warrants a new assessment to ascertain whether the crashworthiness of the associated dynamic structural response provides an equivalent or improved level of safety compared to conventional metallic structures. Generally, this assessment includes the evaluation of the survivable volume, the retention of items of significant mass, deceleration loads experienced by the occupants, and occupant emergency egress paths. Keeping these requirements in mind in order to design, evaluate, and optimize the crashworthiness behavior of composite structures necessitates development of analytical methods and predictive computational tools. With that objective, NIAR used LS-DYNA® to develop a numerical model of the Boeing 737 10-ft section, as drop tested by the FAA. The 10-ft fuselage section geometry and material properties were reverse-engineered using repair manuals, design books, and documentation provided by the FAA. The FE model followed NIAR methodologies and mesh quality criteria. The occupants and seats were represented using mass elements. Items of mass such as lifting fixtures, camera mounts, reinforcing beams, and overhead bins were represented using finite elements. Additionally, the luggage was also incorporated into the FE model, and several studies were performed in order to accurately represent its aggregate mechanical properties. During the validation process, it was found that some geometry simplifications did not provide an adequate level of correlation. Thus, the sensitivity of increased accuracy in the geometric representation was also studied in order to provide guidance on the minimum geometric features necessary to capture the event. The final 10-ft fuselage section model was validated by comparing floor accelerations and velocities, as well as fuselage permanent deformations. A good level of correlation was obtained from this analysis, which shows that numerical methods can be used to support the design and certification of future aircraft structures for crashworthiness evaluation.*

**Keywords:** Crashworthiness, Aircraft Structures, Numerical Methods, Drop Test, Boeing 737, FAA, LS-DYNA

## Introduction

The FAA requires an assessment of each new aircraft design regarding crashworthiness performance. In addition, the introduction of composite airframes warrants a new assessment of crashworthiness in order to determine that the dynamic structural response provides an equivalent or improved level of safety, compared to conventional metallic structures. A significant amount of work on metallic aircraft structures has been previously conducted; however, there is a lack of data in the public domain on the crashworthiness behavior of composite aircraft structures. To design, evaluate, and optimize the crashworthiness behavior of composite structures, it is necessary to develop analytical methods and predictive computational tools.

Due to the high cost and unavailability (for testing) of full scale aircraft, often only sub-assemblies of an aircraft are structurally tested. In this paper, a 10-ft. fuselage section (FS) including the cargo door was extracted from NIAR's full aircraft CAD model, and compared to the 10-ft. FS from a Boeing 737 drop test conducted by the FAA [2]. NIAR's analytical results of the 10-ft. FS, with cargo, were compared against the FAA test results to corroborate that the FE model behavior and response were within a reasonable range of the experimental test results [2]. Good correlation between test and simulation data was observed based on the comparison of

deformations, accelerations, and velocities. The validation of 10-ft FE model is the necessary and required step before validating the full scale aircraft, which can help to better understand its crashworthiness characteristics.

### CAD Model Description

The FAA test discussed above involved a 10-ft fuselage section extracted from a Boeing 737-100 (B737) classic series aircraft. From literature review, the tested fuselage section from FS 380- FS 500 is found to be common across all B737 models. The section, including the cargo door, is shown in Figure 1[2]. A 10-ft. FS was extracted from the full aircraft CAD model of NIAR’s narrow body aircraft model at the same location as that of the FAA test. Besides main structural components, the overhead bins, lifting plates, and camera mounts were also defined in NIAR’s 10-ft FS model. Due to the lack of manufacturer engineering drawings, the CAD model was reverse engineered based on information in repair manual [4], publications [5], and FAA documentations[1][2].

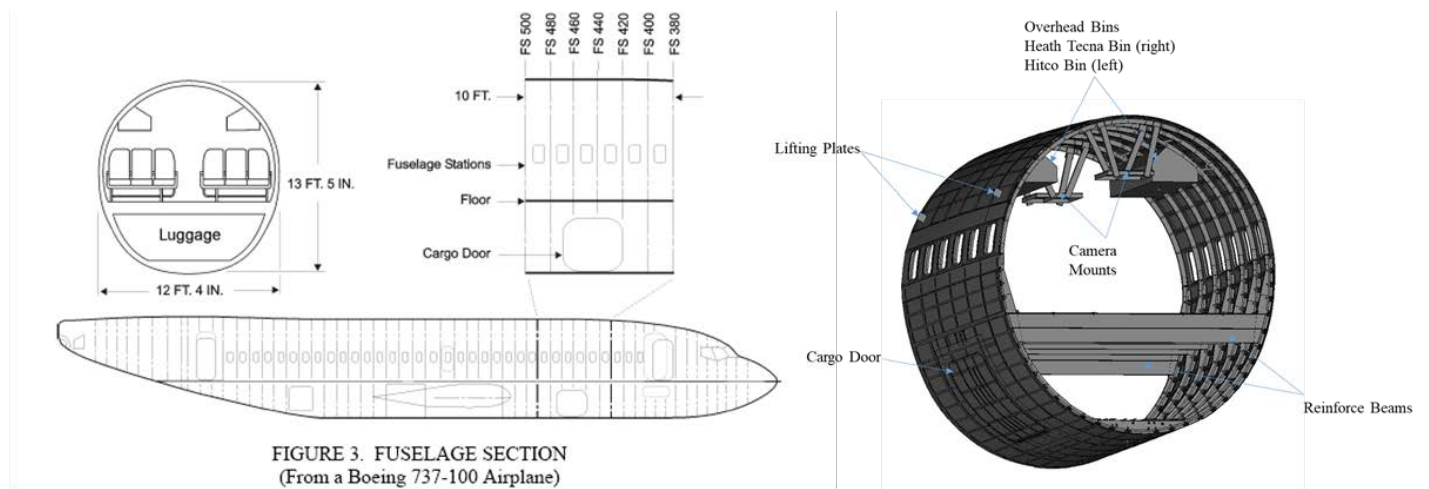


Figure 1. 10-ft. Section Extraction Location from Full Aircraft – FAA Test (Left) and NIAR CAD Model (Right)

### FE Model Development

#### FE Model Definition

Structural parts of the airframe, as well as reinforcement beams, camera mounts, and lifting plates, were discretized (meshed) using shell elements. Table 1 shows total numbers of solid, shell, beam, and lumped mass elements. Mesh quality criteria in Table 2 was applied to the all 2D and 3D elements in the model. All initial penetrations and intersections greater than 0.1 mm were eliminated.

Table 1. Number of Element Entities

|                       | Total Number |
|-----------------------|--------------|
| <b>Nodes</b>          | 827633       |
| <b>Lumped masses</b>  | 32           |
| <b>Beam Elements</b>  | 24660        |
| <b>Shell Elements</b> | 669039       |
| <b>Solid Elements</b> | 25080        |

Table 2. Mesh Quality Criteria

| Quality Parameter | 2D Elements | 3D Elements |
|-------------------|-------------|-------------|
| Min. Side Length  | 5 mm        | 5 mm        |
| Max. Aspect Ratio | 5           | 5           |
| Min. Quad Angle   | 45 deg      | 45 deg      |
| Max. Quad Angle   | 140 deg     | 140 deg     |
| Min. Tri Angle    | 30 deg      | 30 deg      |
| Max. Tri Angle    | 120 deg     | 120 deg     |
| Max Warp Angle    | 15 deg      | 15 deg      |
| Min. Jacobian     | 0.7         | 0.5         |
| Tet Collapse      | N/A         | 0.3         |

### ***Connections***

Connections between the structural parts were modeled by Mesh-Independent Spot-weld Beams. In this modeling approach, connections can be placed at arbitrary location with respect to the element since they do not require nodal connectivity. The spot-weld beam elements are attached to the elements by a tied contact. Due to the scale of the problem this was the most practical way of representing the connections [7].

### ***Material***

The floor panels were modeled as elastic material (MAT\_001). The metallic parts of the airframe structure as well as reinforcement beams and camera mounts were modeled using an isotropic elasto-plastic material model (MAT\_024) in LS-DYNA. Failure criteria was defined using plastic failure strains. All the material data for metallic parts was extracted from MMPDS [6].

### ***Contacts and Constraints***

Contact between structural parts was defined using \*CONTACT\_AUTOMATIC\_SINGLE\_SURFACE card. \*CONTACT\_AUTOMATIC\_SURFACE\_TO\_SURFACE card was defined between cargo and surrounding structure, and \*CONTACT\_AUTOMATIC\_SINGLE\_SURFACE card was defined between the cargo pieces. In order to prevent negative volume, \*CONTACT\_INTERIOR was applied to the solid elements in the cargo. The cargo door was connected to the surround structures by \*CONSTRAINT\_NODAL\_RIGID\_BODY.

### ***Cargo***

NASA performed a quasi-static compression test of four vertically stacked bags and obtained an equivalent material stress and strain curve [3]. Following the Building Block Approach, NIAR did the component level validation for the luggage by conducting similar quasi-static analysis as shown in Figure 2. The simulation result agreed well with the test data as shown in Figure 3.

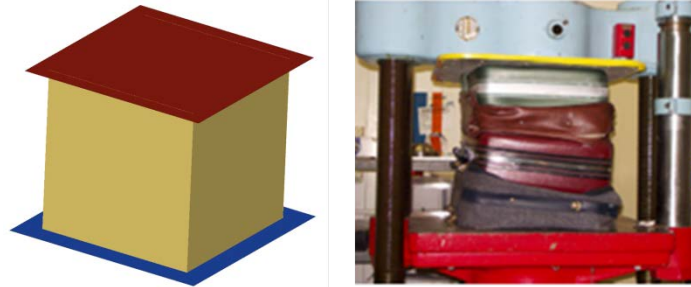


Figure 2. NIAR Luggage Crush Test (Left) and NASA Luggage Crush Test (Right)

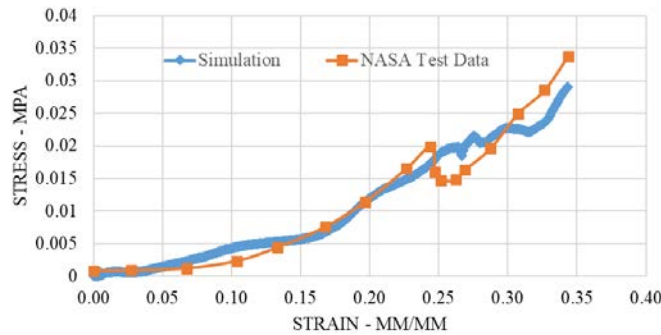


Figure 3. Stress vs Strain Curve from NIAR Simulation Comparing with NASA Test Data

Based on images of the test setup shown in Figure 4, the luggage in the front and rear were different in number and sizes, which indicated that the luggage was distributed randomly. Initially, it was not known if modelling the cargo as a single piece - or multiple pieces - would yield more accurate results. Thus, two simulations comparing these different scenarios were conducted. As seen in Figure 5, the acceleration response from the right inner and outer seat track of the cargo with multiple pieces was more representative of the actual test data. As a result, cargo was modelled in multiple pieces. As an attempt to emulate the FAA test luggage as close as possible, the FE cargo model was divided into 84 pieces to simulate movement and shifting of bags as shown in Figure 6. The cargo was discretized using solid elements, and the material card \*MAT\_CRUSHABLE\_FOAM (MAT\_063) was used to simulate the material response.

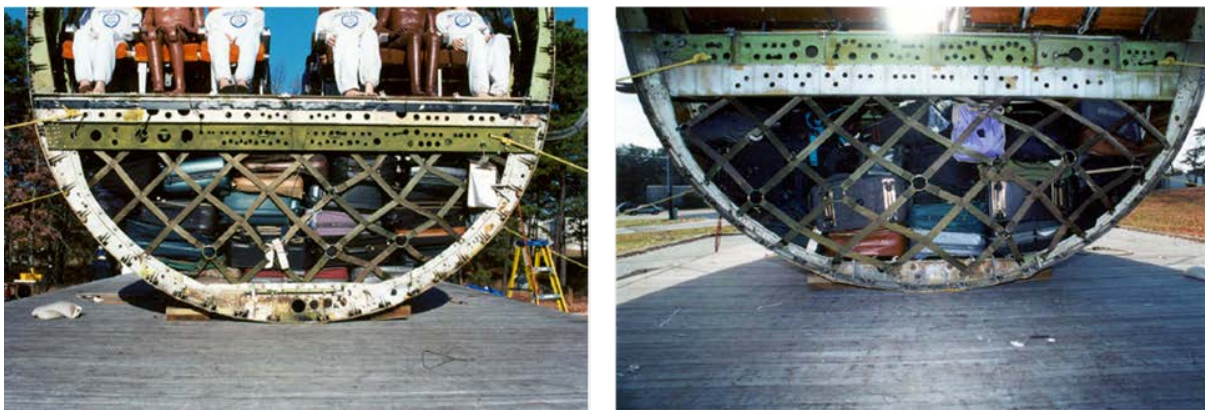


Figure 4. Cargo Area- Luggage, Front (Left) and Luggage, Rear (Right)

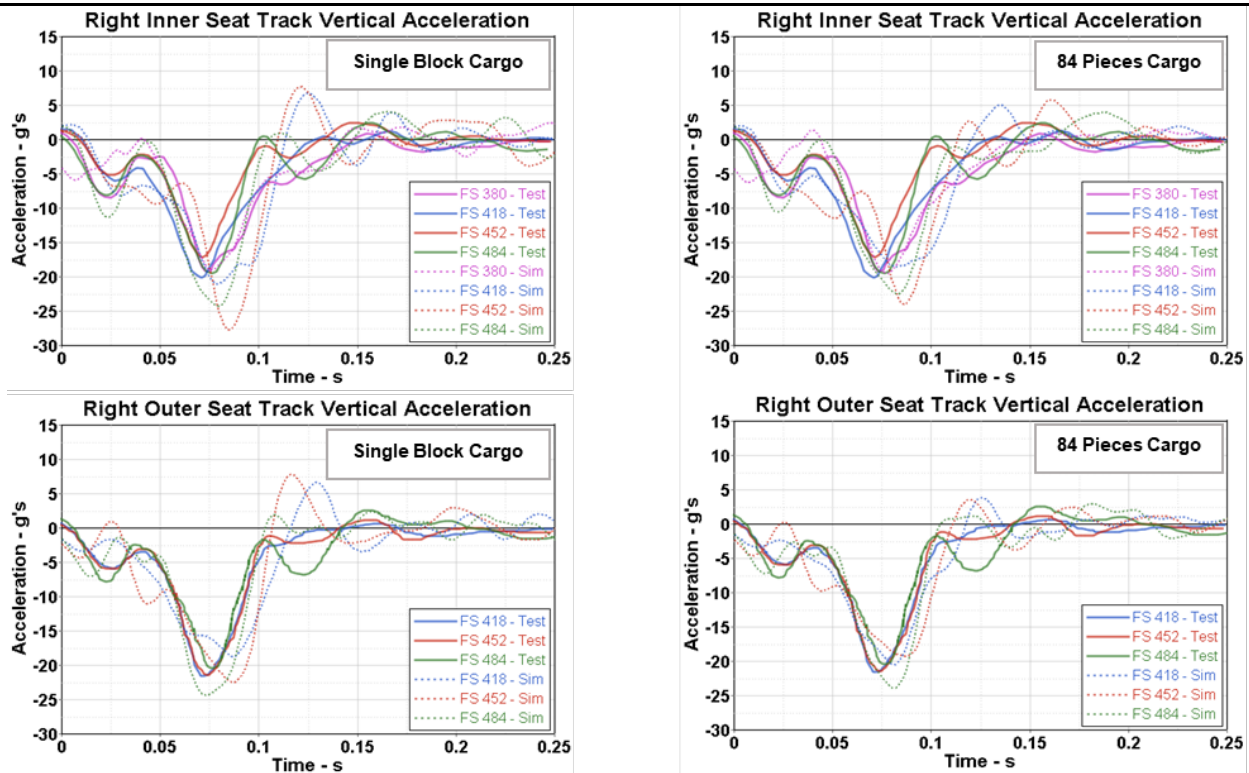


Figure 5. Right Seat Track Floor Accelerations of 10-ft FS Comparing Simulations with Single Block Cargo (Left) and 84 Pieces Cargo (Right) to FAA Test

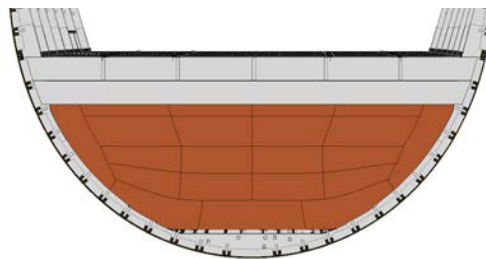


Figure 6. Luggage 84 Pieces Cargo FE Model

**Overhead Bins**

The tested 10-ft fuselage section was equipped with two overhead stowage bins; a Hitco bin at the left side and a Heath-Tecna bin at the right side. Strain gages were installed on support structures of the bins. The bin sizes were determined based on the mounting locations diagram of the support structures. Bin contents were represented as lumped masses, to match the C.G. locations on the test, which were determined from load distribution data of static calibrations [2].

**FE Model Set Up**

**Weight Balance**

Each of the 6 passenger seats - with its occupants (1 ATD and 2 Mannequins) - were represented by 4 lumped masses. These masses were attached to the seat tracks at the same location the actual seat legs were. The cameras' weight was evenly applied at the camera mounting plates. The switch box and the miscellaneous mass, together with the differential between the mass of the fuselage structure model and actual test article, were

applied at the four corners of passenger floor. The locations of the lumped masses are shown in Figure 7. Table 3 shows the overall mass distribution of the complete set-up.

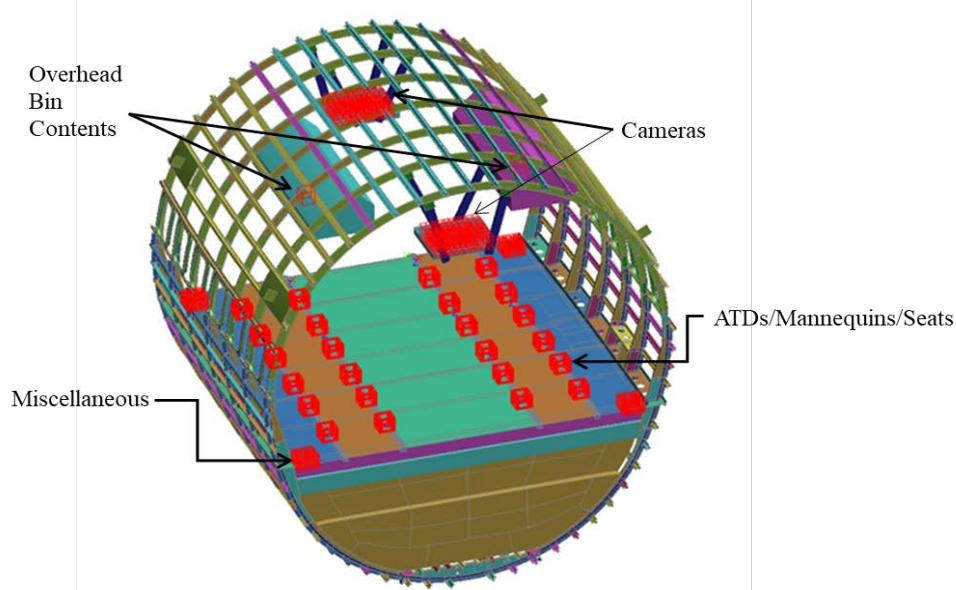


Figure 7. Lumped Masses on FE Model for Seats, ATDs, Overhead Bins, and Camera

Table 3. Weight Summary and Comparison between FAA Test and NIAR FE Model

|    | Item                      | FAA Report   |          |             |                | Overall (kg)   | FE model (kg)  |
|----|---------------------------|--------------|----------|-------------|----------------|----------------|----------------|
|    |                           | Weight (lbf) | Quantity | Total (lbf) | Total (kg)     |                |                |
| 1  | ATD                       | 170          | 3        | 510         | 231.33         | 778.36         | 778.36         |
| 2  | Mannequin                 | 161          | 6        | 966         | 438.17         |                |                |
| 3  | UOP Seat                  | 80           | 3        | 240         | 108.86         |                |                |
| 1  | ATD                       | 170          | 3        | 510         | 231.33         | 762.03         | 762.03         |
| 2  | Mannequin                 | 161          | 6        | 966         | 438.17         |                |                |
| 4  | Weber Aircraft Seat       | 68           | 3        | 204         | 92.53          |                |                |
| 5  | Heath Techna Bin (empty)  | 56           | 1        | 56          | 25.40          | 79.83          | 79.83          |
| 6  | Heath Techna Bin Contents | 120          | 1        | 120         | 54.43          |                |                |
| 7  | Hitco Bin (empty)         | 57           | 1        | 57          | 25.85          | 116.57         | 116.57         |
| 8  | Hitco Bin Contents        | 200          | 1        | 200         | 90.72          |                |                |
| 9  | Fuselage                  | 1360         | 1        | 1360        | 616.89         | 616.89         | 616.89         |
| 10 | Luggage                   | 3229         | 1        | 3229        | 1464.65        | 1464.65        | 1464.65        |
| 11 | Camera Mount              | 70           | 2        | 140         | 63.50          | 63.50          | 63.50          |
| 12 | Cameras                   | 22           | 4        | 88          | 39.92          | 40.00          | 40.00          |
| 13 | Switch Box                | 7            | 1        | 7           | 3.18           | 3.18           | 101.61         |
| 14 | Miscellaneous             | 217          | 1        | 217         | 98.43          | 98.43          |                |
|    | <b>Total</b>              |              |          | <b>8870</b> | <b>4023.36</b> | <b>4023.36</b> | <b>4023.45</b> |

## Accelerometer Locations

In order to compare vertical accelerations of cabin floor with test data, 14 accelerometers were installed on the seat tracks using \*ELEMENT\_SEATBELT\_ACCELEROMETER. These accelerometers were located at FS380, FS418, FS452, FS484 on the inner seat tracks for both left side and right side, and FS418, FS452, FS484 on the outer seat tracks for both left side and right side. The locations were based on those found on the test article [2].

## Results and Discussion

In this section, the results of the validation run are compared to those of the FAA test in terms of kinematic frames, accelerations, and deformations. The set-up of the validation run was described in the previous section. Through the validation process, it was discovered that certain geometric details needed to be represented correctly for obtaining good correlation of deformations and accelerations. These findings are also documented in this section.

### *Kinematic Frames*

Figure 8 shows a comparison of kinematic frames between the FAA test and the simulation results. At first, the subfloor structure of the fuselage section of the physical test deformed evenly. Then, after 60 ms, the left side of the subfloor structure collapsed more than the right side, and the floor beams started to tilt to the left side. At 150 ms, buckling was observed at the right top portions of the frames. Overhead bins remained attached to the frames during the test. The numerical analysis successfully captures these behaviors of the physical test.

The FE luggage model had a constant stiffness, while the scattered luggage in the FAA test may have had different stiffness values at different locations. This may explain some of the differences in deformations of the lower part (cargo subfloor) of the fuselage.

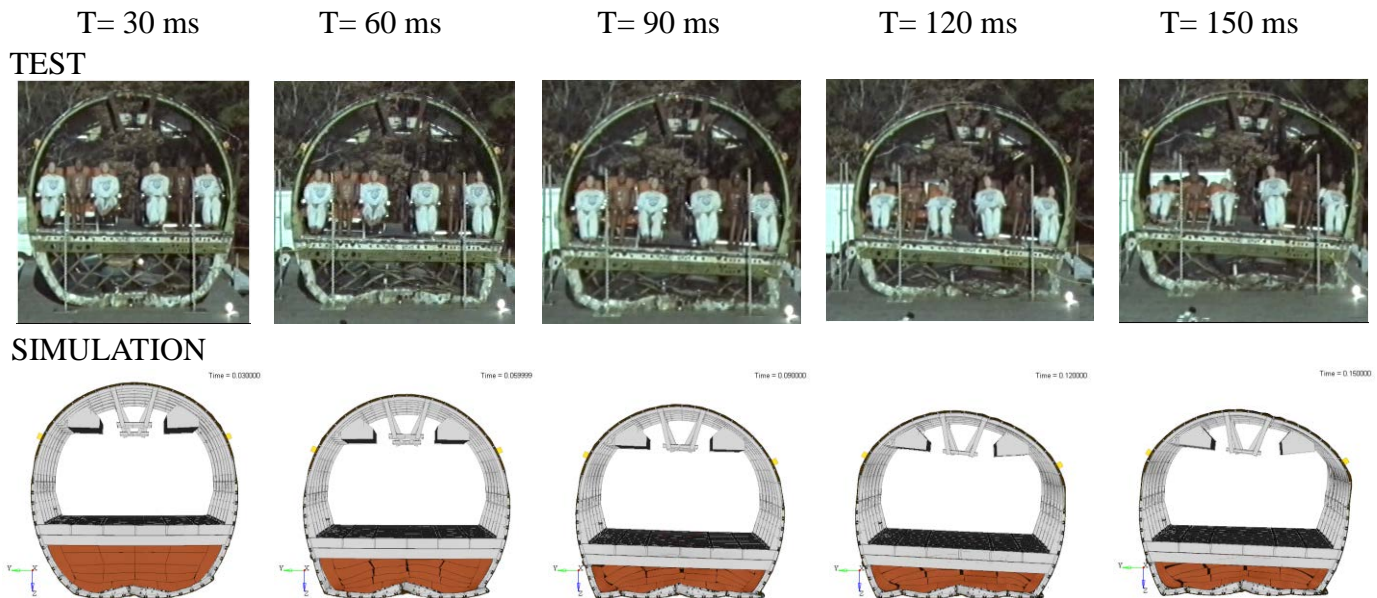


Figure 8. Kinematic Frames of 10-ft FS Comparing Simulation to FAA Test

### *Accelerations and Velocities*

The velocities were output from the accelerometers data. By taking a derivative of the velocities, acceleration time histories of the simulation were obtained. The same SAE J211 20 Hz filter used during the physical drop test [2] was used to filter the numerical acceleration data. The numerical analysis results well represent the value and timing of the drop test accelerations. Considering the assumptions in geometry, connections, and

FEM set-up due to cargo, very good correlation of acceleration data was obtained as shown in Figure 9 and Figure 10.

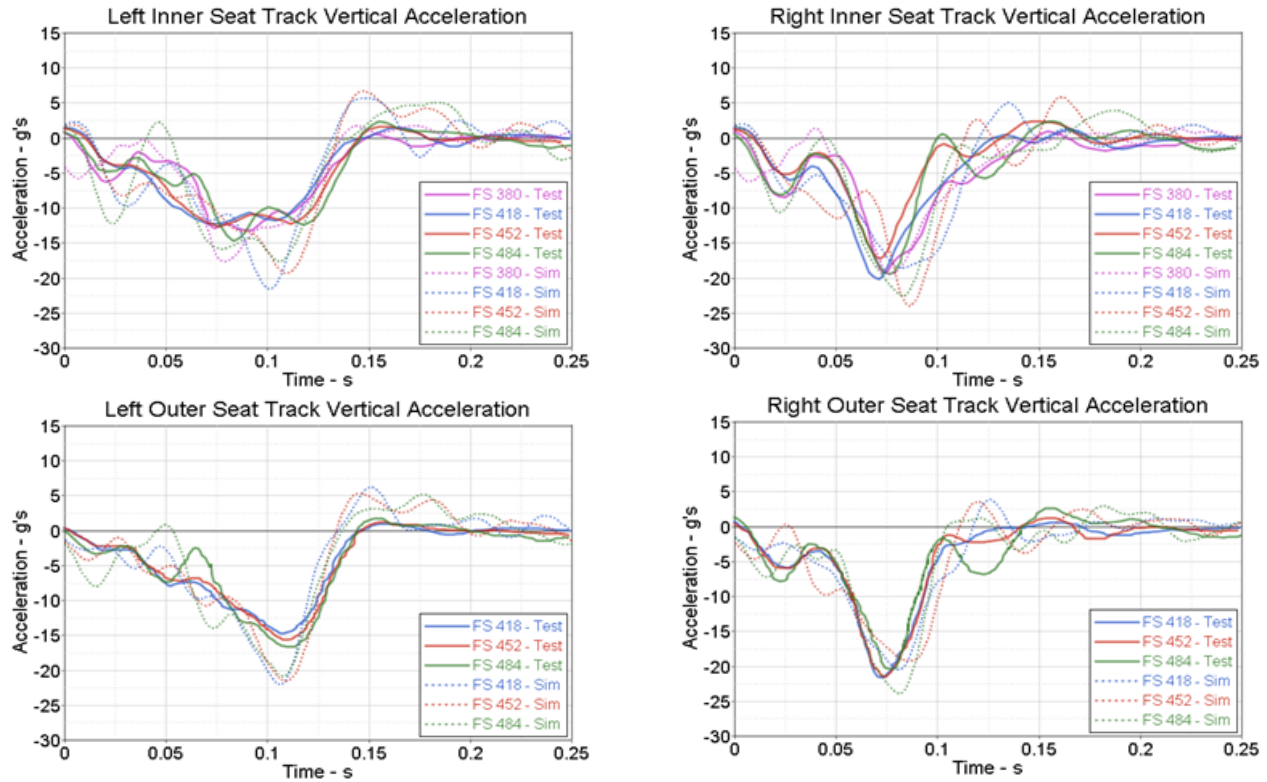


Figure 9. Floor Accelerations of 10-ft FS Comparing Simulation to FAA Test

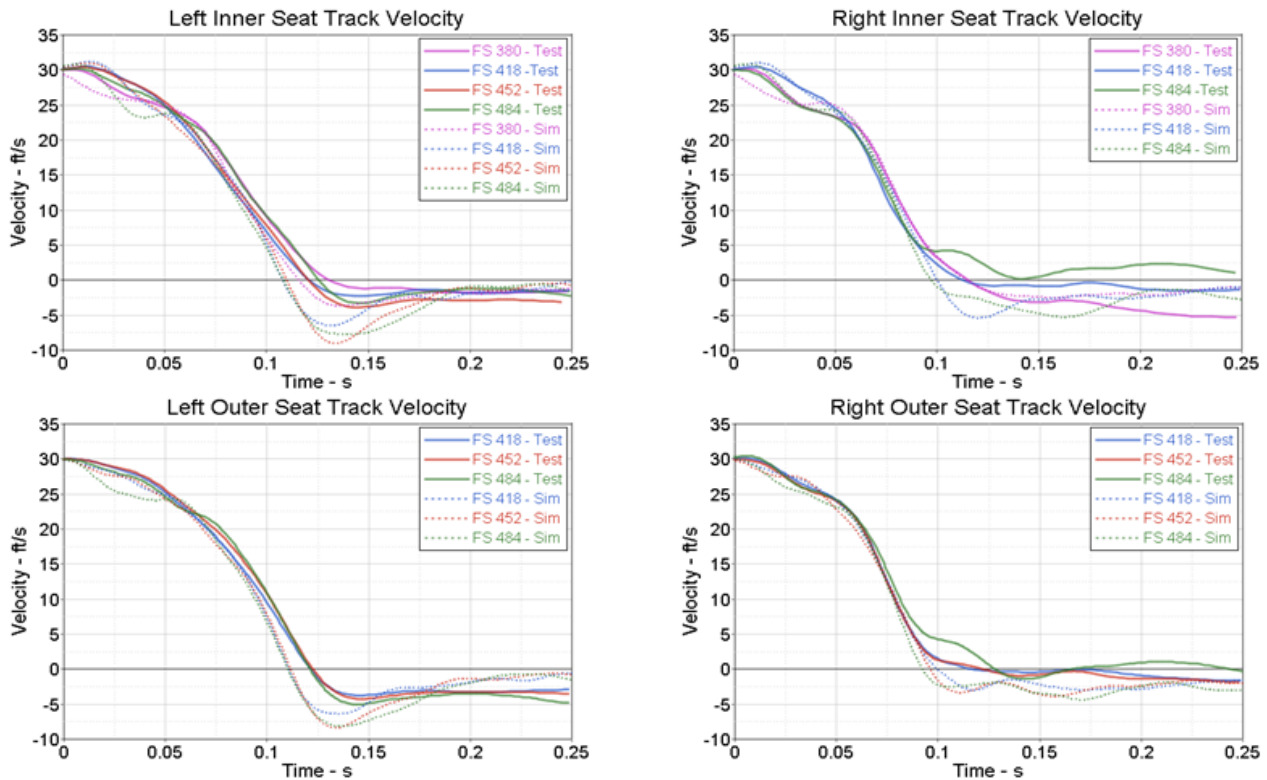


Figure 10. Floor Velocities of 10-ft FS Comparing Simulation to FAA Test

**Deformation Comparisons**

This section compares the deformations in the FE model to those observed in the physical test [1]. The front and back views of deformations are shown in Figure 11. The deformations in the inner structure, cargo floor, and frames are shown in Figure 12. These deformations show similar mode of failure in both the physical test and the FE model, even though localized differences exist. One of the factors contributing to these differences could be the cargo response on the FE analysis. As noted in the previous section, the luggage in the test was loosely packed and may have varying stiffness across the fuselage. On the contrary, the cargo in the numerical model had a constant stiffness value based on the component level results.

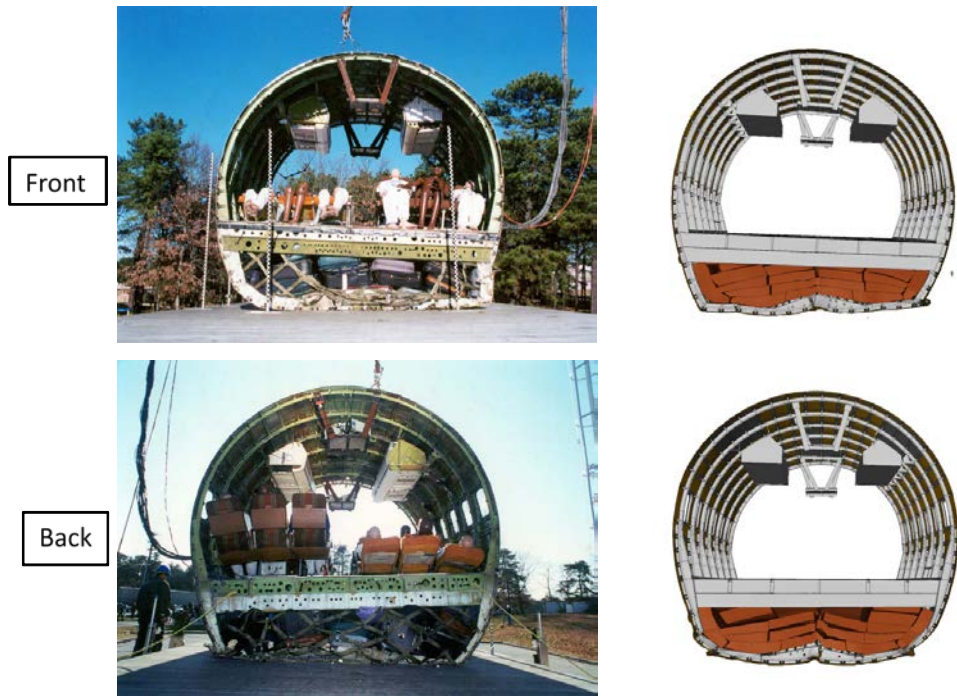


Figure 11. Front and Back View Deformation Comparison between Test and Simulation

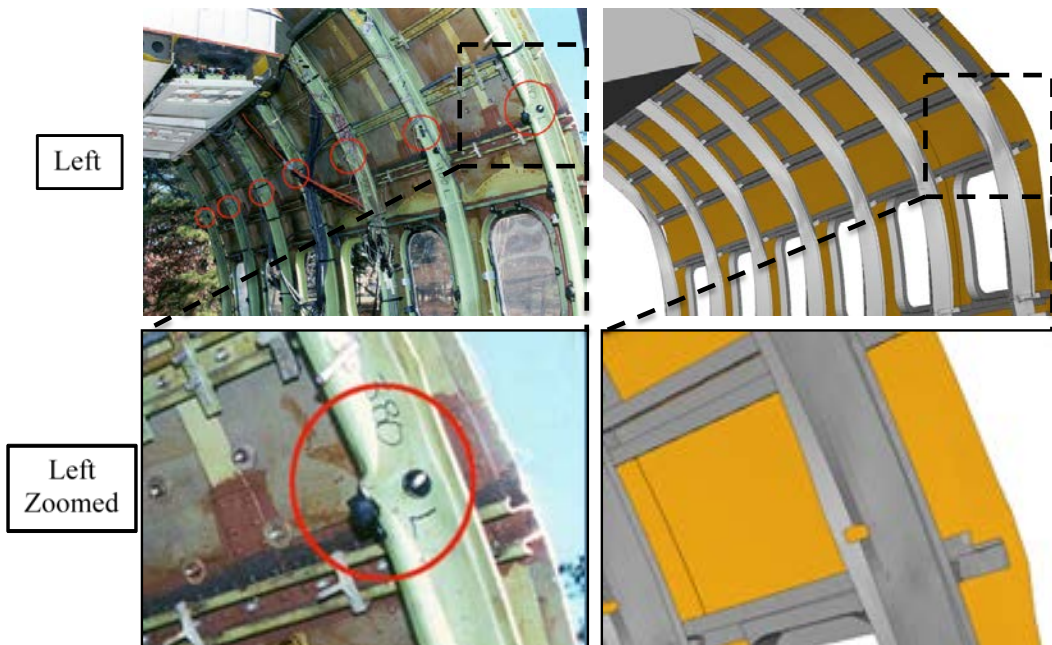


Figure 12. Left View Upper Frames Deformation Comparison between Test and Simulation

### Effect of Geometric Details

Throughout the study, it was realized that geometric details can have huge effects towards the outcome of the simulations. As such, different studies were conducted to better understand the sensitivity of the geometric details, in order to determine the minimum geometric representation required to capture the deformations seen in the test.

In the initial simulations, the lower frames were simplified by omitting the lightening holes. The simplification resulted in a different mode of failure, when compared to the FAA test (see Figure 13). A closer examination of FAA test revealed that there were cracks initiated at the lightening holes, which led to the frames' failure. Once, the lightening holes were added to the FE model as shown in Figure 14, the simulation results showed a better correlation with the physical test (see Figure 15).

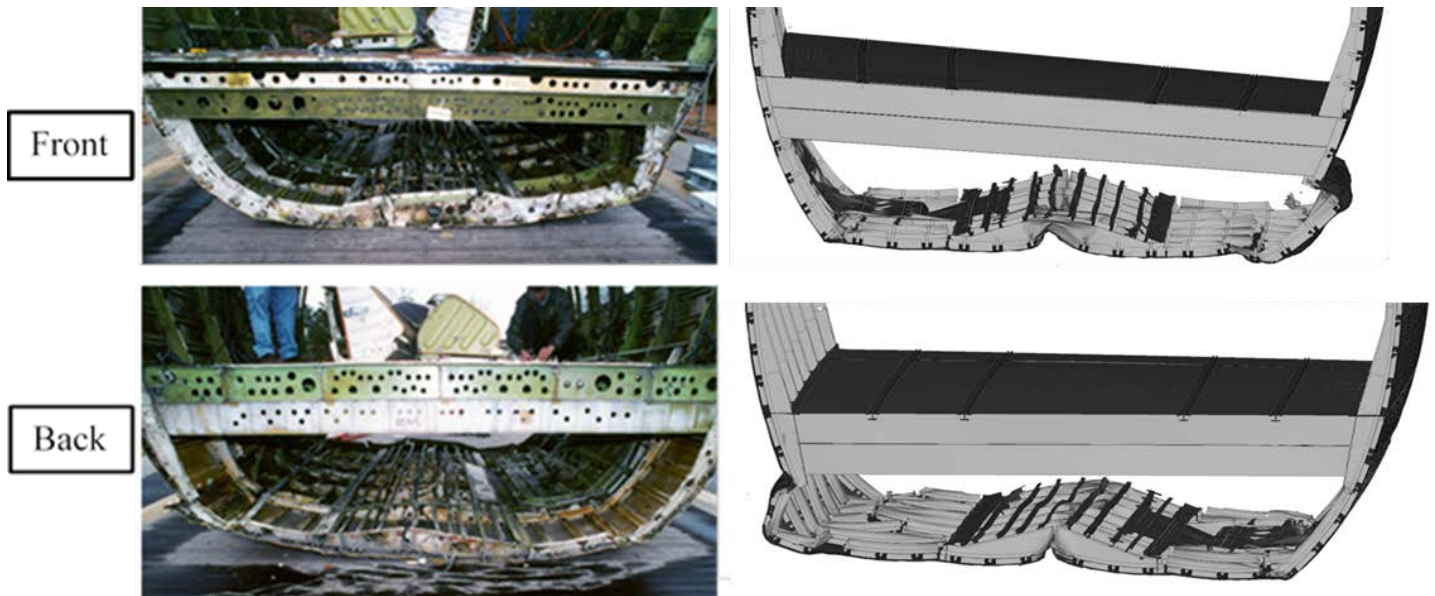


Figure 13. Front and Rear View Lower Frames Comparison between Test and Simulation without Lightening Holes

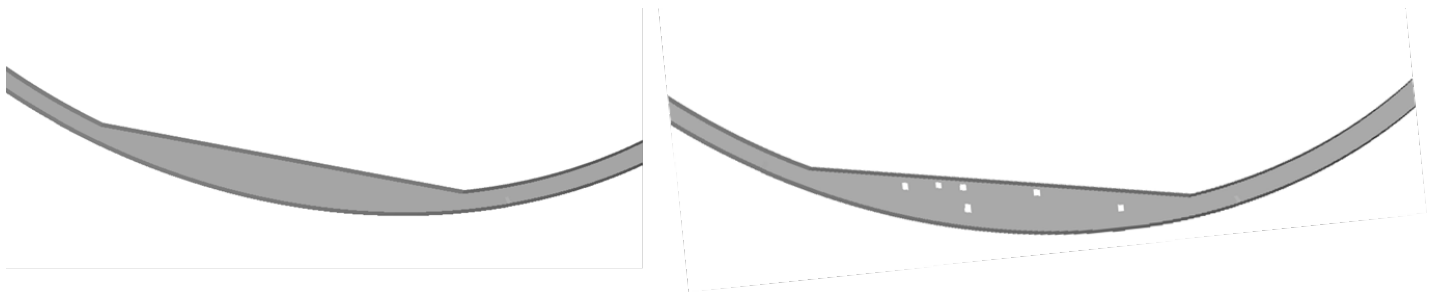


Figure 14. Lower Frame without Lightening Holes (Left) and Lower Frame with Lightening Holes (Right)

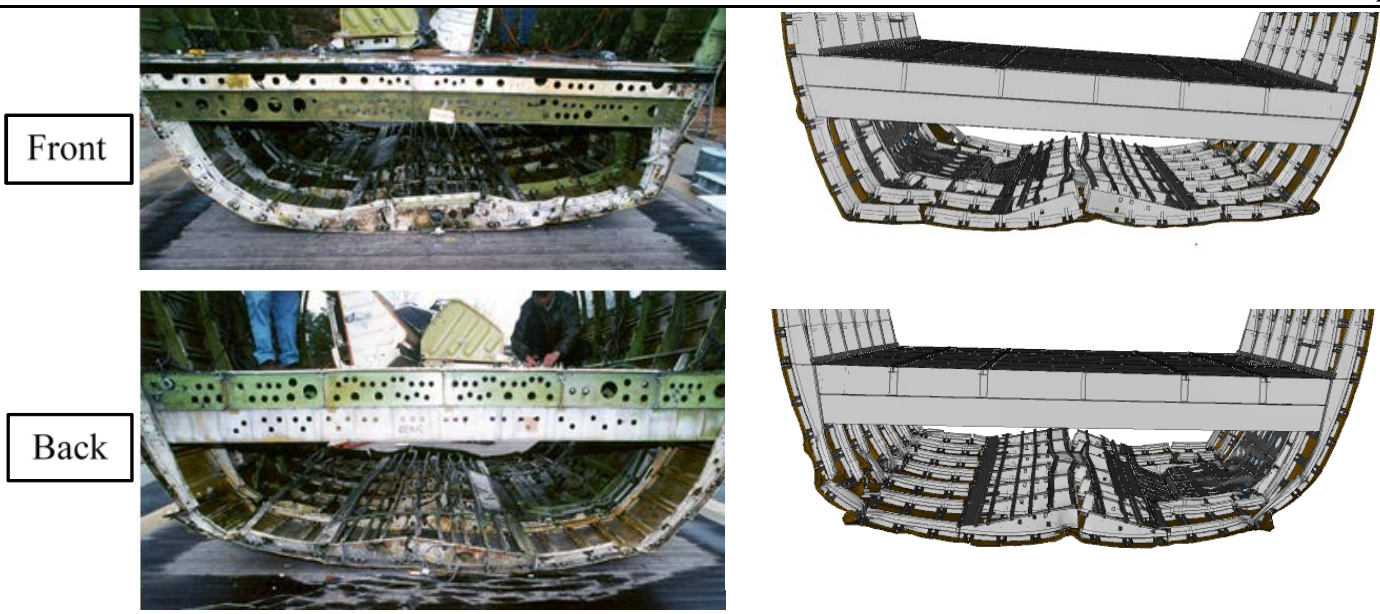


Figure 15. Front and Rear View Cargo Floor Deformation Comparison between Test and Simulation with Lightening Holes

Obtaining accurate acceleration response was important since it directly affects the occupant response. Two important components with great influence on acceleration response are the floor and floor beams. Because the floor beams' geometry was assumed, a study on the floor beam stiffness was conducted. As shown in Figure 16, the numerical model with the stiffened floor beam geometry showed a better correlation to the test data than the original geometry. This highlights the importance of having the right geometry and material information. However, since there is no evidence to support the incorporation of this stiffened beam, the original beam was used for the final validation analysis.

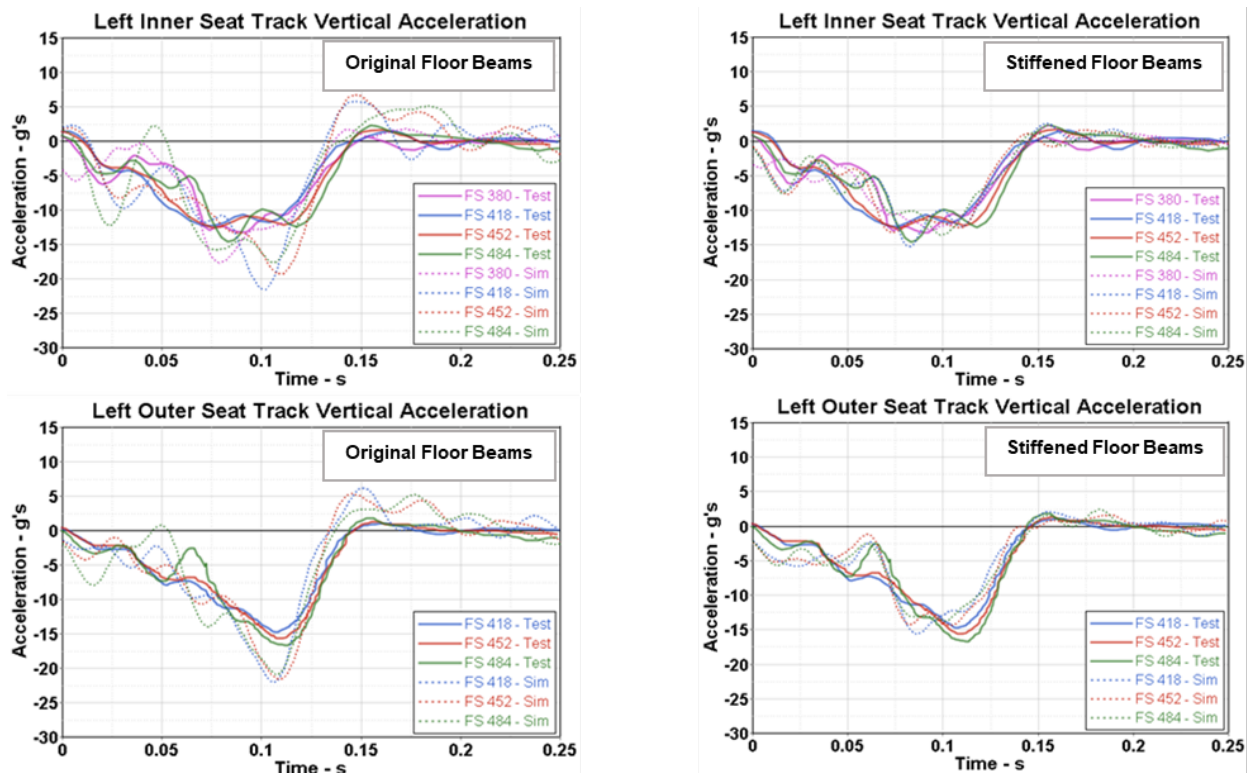


Figure 16. Left Seat Track Floor Accelerations of 10-ft FS Comparing Simulations with Less Stiffened Floor Beams (Left) and more Stiffened Floor Beams (Right) to FAA Test

## Conclusion

The NIAR 10-ft FS model was analyzed and compared to the Boeing 737 10-ft FS vertical drop test data and results as conducted by FAA. The FE model was set up such that all the masses (cargo, overhead bins, occupants and seats, etc.) matched the masses on the test article. Due to limited engineering and manufacturing data, the fuselage structure, materials, and fasteners on the analytical model were not identical to the test article. A uniform stiffness value was assigned to the cargo representation used in the FE model. It's assumed that the actual physical cargo stiffness was not uniform, and varied greatly between locations because of different types of bags distributed in the cargo bay. The kinematic frames, acceleration and velocity time histories, and the deformations were compared to the test.

Although there are differences in the peak acceleration values, phase of some of the acceleration plots, and deformation patterns, overall a good correlation of the numerical analysis to the test was observed. This proves that current FE software has the capability to solve complex non-linear dynamic simulations such as this subject 10-ft FS drop. Any discrepancies revealed were mostly the result of geometric assumptions, which had been found to have large effect on the simulation results. Thus, analytical results could be improved, with net simulation results closer to those seen on the physical test, if detailed information from the physical test about the geometry, materials, fasteners, and boundary conditions were made available.

## References

- [1] Abramowitz, A., "Summary of the FAA's Overhead Stowage Bin Crashworthiness Program", FAA Report DOT/FAA/AR-99/4, 2010.
- [2] Abramowitz, A., Smith, T. G., Vu, T., and Zvanya, J. R., "Vertical Drop Test of a Narrow-Body Transport Fuselage Section with Overhead Stowage Bins", FAA Report: DOT/FAA/AR-01/100, 2002.
- [3] Jackson, K. E., and Fasanella, E. L., "Crash Simulation of Vertical Drop Tests of Two Boeing 737 Fuselage Sections", FAA Report: DOT/FAA/AR-02/62
- [4] 737-800 Structural Repair Manual, The Boeing Company, 2013.
- [5] Niu, C. Y., *Airframe Structural Design*, Conmilit Press Ltd., 1993.
- [6] FAA Report DOT/FAA/AR-MMPDS-09: *Metallic Materials Properties Development and Standardization*, April 2014.
- [7] C. Zinzuwadia, "Finite Element Modeling of a Single Shear Fastener Joint Specimens: A Comparison of Simplified Joint Modeling Techniques," Master's Thesis, Wichita State University, 2014.
- [8] Federal Register: June 11, 2007 (Volume 72, Number 111), Proposed Rules, Page 32021-32023, Federal Register Online via GPO Access <http://www.access.gpo.gov/http://edocket.access.gpo.gov/2007/E7-11153.htm>